

SURFACE VISCOSITY MEASUREMENTS FROM LARGE BILAYER VESICLE TETHER FORMATION

I. ANALYSIS

RICHARD E. WAUGH

Department of Radiation Biology and Biophysics, University of Rochester, School of Medicine and Dentistry, Rochester, New York 14642

ABSTRACT Recent observations indicate that it is possible to form tethers from large phospholipid vesicles. The process of tether formation is analyzed using a continuum mechanical approach to obtain the surface viscosity of the bilayer in terms of experimentally measurable parameters. The membrane is treated as a two-dimensional isotropic material which deforms at constant area. The constitutive equation relates the maximum surface shear resultant to the rate of deformation via the surface viscosity coefficient. The force which acts to increase the tether length is generated by fluid moving past the vesicle. The magnitude of the force is estimated from Stokes's drag equation. The analysis predicts that there is a critical force necessary to produce an increase in the tether length. A dimensionless tether growth parameter is defined, and its value is obtained as a function of the ratio of the applied force on the vesicle to the critical force. This relationship is independent of both the size of the vesicle and the radius of the tether. Knowing the force on the vesicle, the critical force, and the rate of tether growth, the surface viscosity can be calculated.

INTRODUCTION

Biological membranes behave as two-dimensional materials. Strictly speaking, they can be considered as continuous only in the two dimensions of the surface, with a molecular character in the direction normal to the surface. The erythrocyte membrane has served as a model system for the study of such materials, and the continuum mechanical properties of erythrocyte membrane have been characterized. (See Evans and Skalak, 1980, for a thorough review.) The application of material science to other types of membrane has been slow, largely because of the existence of cytoplasmic structures in most cells which, at best, complicate the mechanical analysis and, at worst, dominate the behavior of the cell in deformation. The mechanical behavior of any membrane reflects the composite properties of the membrane constituents. Therefore, an alternative approach to the study of membrane mechanics is to study the properties of reconstituted membrane components to ascertain the contribution of each constituent. The phospholipid bilayer is a major constituent of virtually all biological membranes, and it is with the bilayer that the study of membrane components logically begins.

Recently, it has been observed that large multilamellar phospholipid bilayer vesicles can become attached to glass surfaces and form tethers between the point of attachment and the body of the vesicle (E. Evans and R. Kwok, University of British Columbia, personal communication).

Similar tethers have been observed when erythrocytes attached to glass surfaces were subjected to fluid shear stress (Hochmuth et al., 1973). Subsequent analysis of erythrocyte tether formation by Evans and Hochmuth (1976) led to the determination of the plastic viscosity coefficient for erythrocyte membrane. The observation of tether formation from vesicles prompted the hope that analysis of this process might lead to a new approach to the measurement of the viscosity of a phospholipid bilayer. It was with this end in mind that this analysis was undertaken.

ANALYSIS

Description of the Problem

A vesicle forming a tether of radius, r_t , is illustrated schematically in Fig. 1. The tether radius in the figure is exaggerated; for the purposes of analysis it is assumed to be much smaller than the size of the vesicle. The origin of the cylindrical coordinate system, (r, ϕ, z) , is fixed at the center of the vesicle. The dimension, R_s , is the maximum value of the coordinate, r . The surface coordinate, s , represents the distance along a meridian in the surface from the plane $z = 0$. The angle, θ , is the angle between the surface tangent and the z -axis. Fluid moving past the vesicle exerts a drag force, F , on the vesicle in the z -direction. The pressure inside the vesicle, P_i , is greater than the pressure outside the vesicle, P_o , and the differ-

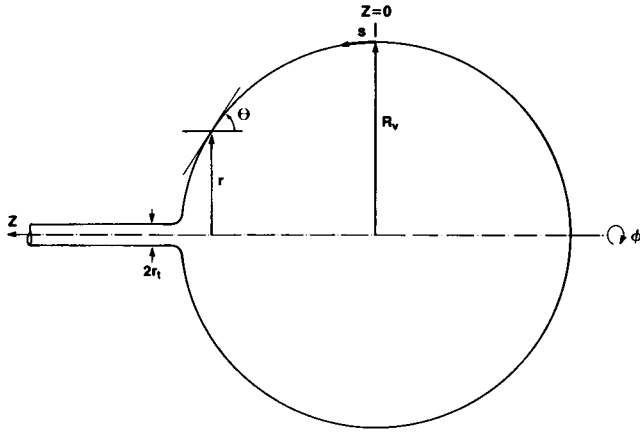


FIGURE 1 Schematic of a vesicle forming a tether, showing major dimensions and coordinates. The origin of the cylindrical coordinate system (r, ϕ, z) is at the center of the vesicle. The maximum radial dimension is R_v , and the tether radius is r_t . The distance along a meridian in the surface is s , and the angle between the surface tangent and the z -axis is θ .

ence, $\Delta P = P_i - P_o$, is assumed to be constant. Material in the tether is drawn from the body of the vesicle. The velocity of the material relative to the origin, v_m , is a function of the radial position, r . The radius of the tether is assumed to be constant over its length, and the material velocity in the tether is uniform. No assumptions are made about the shape of the vesicle surface, except that it is axisymmetric about the z -axis.

The force resultants in the surface are called tensions and have units of dynes per centimeter. The principal tensions are T_m and T_ϕ , the former acting in the direction of the surface coordinate, s , and the latter acting perpendicular to T_m . Two equations that describe the balance of forces in the system can be applied. The first is a tangential force balance in the meridional direction (Evans and Skalak, 1980, Eq. 3.5.9):

$$r \frac{dT_m}{ds} + (T_m - T_\phi) \frac{dr}{ds} + r\tau = 0. \quad (1)$$

The second is a balance of forces in the z -direction:

$$T_m(2\pi r \cos \theta) - [F \int_{r_t}^r (\tau \cos \theta + p \sin \theta) (2\pi r) dr] - \Delta P(\pi r^2) = 0. \quad (2)$$

Acceleration terms are neglected. The quantities, τ and p , represent the tangential and normal stresses exerted on the surface by the moving fluid (i.e., in excess of the external pressure, P_o). The integral in Eq. 2 evaluated over the entire surface of the vesicle is equal to the total force on the vesicle, F . The contribution from these terms is small in the region where the membrane dissipation is important, and they can be neglected without significantly affecting the results of the analysis (see Appendix).

Neglecting these terms and keeping only the total drag, F , Eqs. 1 and 2 become:

$$r \frac{dT_m}{dr} + (T_m - T_\phi) = 0, \quad (3)$$

and

$$2\pi r T_m \cos \theta = F + \pi r^2 \Delta P. \quad (4)$$

The surface behaves like a two-dimensional liquid. It resists changes in area elastically, and has a very low compressibility (Kwok and Evans, 1981). For the magnitude of the force resultants in these experiments the area can be considered constant. Unlike erythrocyte membrane, the bilayer has no shear rigidity. When force resultants in the surface are not isotropic, the surface deforms with a rate of deformation that is proportional to the shear resultant in the surface:

$$T_s = 2\eta V_s. \quad (5)$$

Eq. 5 defines the surface viscosity coefficient, η . The maximum shear resultant in the surface is T_s , and the maximum rate of shear deformation is V_s . In terms of the principal tensions,

$$T_s = \frac{1}{2}(T_m - T_\phi). \quad (6)$$

For an incompressible surface, the rate of deformation can be written in terms of the velocity of a material point in the surface (Evans and Skalak, 1980, section 2.5):

$$V_s = \frac{dv_m}{ds}, \quad (7)$$

where v_m is the velocity of the material in the meridional direction. The force balance equations (Eqs. 3 and 4), the constitutive equation (Eq. 5), and the equation of continuity for a flowing surface (Eq. 14) are the basis for the analysis.

Static Equilibrium

Let us first consider the case where the membrane is in static equilibrium. The rate of deformation of the surface is zero, which means that the maximum shear resultant must also be zero (Eq. 5). Eq. 3 becomes:

$$\frac{dT_m}{dr} = 0. \quad (8)$$

An expression for the tension, T_m , in terms of the force, F , and the pressure, ΔP , is obtained from Eq. 4. Incorporating this result in Eq. 8, we find:

$$\frac{d}{dr} \left(\frac{F}{2\pi r \cos \theta} + \frac{\Delta P r}{2 \cos \theta} \right) = 0. \quad (9)$$

For the boundary condition, we observe that at the rim of the vesicle ($r=R_v$), the cosine must be one ($\cos \theta = 1.0$). Applying this condition to Eq. 9 we obtain a relationship between θ and r which describes the contour of the surface between the point of attachment and the rim of the vesicle in static equilibrium:

$$\cos \theta = \frac{r + F/\pi r \Delta P}{R_v + F/\pi R_v \Delta P}. \quad (10)$$

This expression is approximate because the integral terms in Eq. 2 have been neglected. It is most accurate in the region near the tether ($r \approx r_t$) because the integral terms are smallest there (see Appendix). Observe that when F is zero, Eq. 10 reduces to the spherical case, $\cos \theta = r/R_v$. Also observe that Eq. 10 places limits on the magnitude of the force F . Because $\cos \theta \leq 1.0$,

$$F \leq \pi \Delta P r_t R_v, \quad (11)$$

where r_t is the minimum value of r , or the radius of the tether. For values of the force greater than that in Eq. 11, static equilibrium cannot exist, and the surface must flow. Therefore, we define the critical force,

$$F_o \equiv \pi \Delta P r_t R_v. \quad (12)$$

This is the force at which the tether begins to grow.

Growth of a Tether of Fixed Radius

The differential equation describing the contour of the flowing surface is obtained by combining the constitutive relationship (Eq. 5) with the tangential force balance (Eq. 3):

$$r \frac{dT_m}{dr} + 4\eta V_s = 0. \quad (13)$$

The continuity equation for an incompressible, axisymmetric flowing surface can be written (Evans and Skalak, 1980, p. 43):

$$\frac{d}{ds}(rv_m) = 0. \quad (14)$$

Recalling the expression for the rate of deformation, V_s , in terms of the material velocity, v_m , (Eq. 7) and applying the continuity equation (Eq. 14) we can obtain the following expression for V_s :

$$V_s = \frac{v_m}{r} \sin \theta, \quad (15)$$

where the equality, $dr/ds = -\sin \theta$, has been applied. The material velocity, v_m , is related to the velocity of the vesicle relative to the attachment point, v_v , which is an experimentally observable quantity. The velocity of the vesicle

(v_v) must be equal to the material velocity (relative to the center of the vesicle) at the point, $r = r_t$:

$$v_v = v_m(r_t). \quad (16)$$

Applying the continuity condition (Eq. 14) we can relate the vesicle velocity to the material velocity at any position:

$$v_v = v_m(r) \left(\frac{r}{r_t} \right). \quad (17)$$

Using this relationship in Eq. 15 we find

$$V_s = r_t v_v \frac{\sin \theta}{r^2}. \quad (18)$$

Introducing the axial force balance (Eq. 4) for T_m , and Eq. 18 for V_s , we can write the differential equation for the surface (Eq. 13) as:

$$r \frac{d}{dr} \left[\frac{F}{2\pi r \cos \theta} + \frac{\Delta P r}{2 \cos \theta} \right] + 4\eta r_t v_v \frac{\sin \theta}{r^2} = 0. \quad (19)$$

This expression can be simplified by making the following substitutions and definitions:

$$\begin{aligned} \tilde{r} &= r/r_t \\ y &= 1/\cos \theta \\ F_o &\equiv \pi \Delta P r_t R_v \\ G &\equiv 8\pi\eta v_v/F_o \\ \lambda &\equiv R_v/r_t. \end{aligned} \quad (20)$$

Using these expressions and some algebraic manipulations, we can write Eq. 19 as:

$$\begin{aligned} \frac{dy}{d\tilde{r}} &= \frac{y}{\tilde{r}} \cdot \frac{(F/F_o - \tilde{r}^2/\lambda)}{(F/F_o + \tilde{r}^2/\lambda)} \\ &\quad - \frac{G}{(F/F_o + \tilde{r}^2/\lambda)} \cdot \frac{(y^2 - 1)^{1/2}}{y\tilde{r}^2}. \end{aligned} \quad (21)$$

This is the equation from which the functional dependence of the tether growth parameter, G , on the force ratio, F/F_o , is established. If all of the parameters (F/F_o , G , and λ) are specified, a single boundary condition is sufficient to specify the solution to the equation. By specifying an additional boundary condition, a functional relationship is generated among the three parameters. The boundary conditions are that the angle, θ , be zero at the tether and at the rim of the vesicle, i.e.,

$$y = 1 \text{ at } \tilde{r} = 1, \quad (22a)$$

and

$$y = 1 \text{ at } \tilde{r} = \lambda. \quad (22b)$$

The solution is obtained numerically using a fourth-

TABLE I
G AS A FUNCTION OF F/F_0 , TETHER RADIUS
CONSTANT

F/F_0	$\lambda = 10$	50	500	5,000
1.0	0.00	0.00	0.00	0.00
1.1	0.32	0.31	0.31	0.31
1.3	1.01	0.97	0.97	0.97
1.5	1.76	1.69	1.68	1.68
1.7	2.57	2.46	2.45	2.45
2.0	3.92	3.74	3.72	3.72
2.5	6.54	6.16	6.13	6.13
3.0	9.72	9.02	8.97	8.96
4.0	18.2	16.1	16.0	16.0
5.0	30.2	25.3	25.0	25.0

order Runge Kutta routine. For given values of F/F_0 and λ , the value of G is found which satisfies both boundary conditions simultaneously. When the quantity, λ , is >50 , the functional dependence of G on F/F_0 is insensitive to the value chosen for λ (Table I). The relationship between G and F/F_0 is shown graphically in Fig. 2. For values of $F/F_0 > 3.0$, the value of G is very nearly equal to the square of F/F_0 .

When the force, F , is less than the critical force, F_0 , two solutions exist which satisfy Eq. 21. However, the static solution (Eq. 10) cannot satisfy the two boundary conditions simultaneously except when $F = F_0$. Both conditions can be satisfied, however, if we allow material velocities to be negative, that is, the tether to flow back into the body of the vesicle. Tether resorption, in fact, is observed experimentally.

Tether Radius Dependent on Axial Force

One of the assumptions underlying the analysis so far is that the tether radius, r_t , is independent of the applied axial force, F . Recent work by Hochmuth and Evans

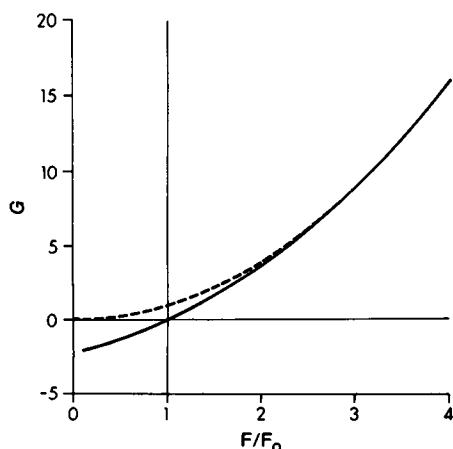


FIGURE 2 Graphic representation of the dimensionless tether growth parameter, G , as a function of the force ratio F/F_0 , assuming the radius of the tether is a constant. The dotted line is the curve $G = (F/F_0)^2$. The function approaches this curve for $F/F_0 \geq 3.0$.

(Duke University, personal communication) indicates that for erythrocyte membrane the tether radius is a function of the axial load. Therefore, it is important to consider what effect such a functional relationship might have on the present analysis. Experimental results are not yet sufficient to prescribe a functional relationship between force and radius. A theoretical derivation is difficult because the membrane cannot be treated as a two-dimensional material since the radius of curvature approaches the thickness of the membrane. Mechanical analysis of the deformation of a thick-walled cylinder of anisotropic material will be required to obtain a proper solution. Such an analysis is beyond the scope of the present work. However, to see what effect a force-dependent tether radius would have on the present analysis, the following inverse relationship will be used:

$$F = \text{const} \cdot \frac{1}{r_t} \quad (23)$$

This relationship is at least qualitatively consistent with what is known and what might be supposed about how the tether responds to an axial force. The radius decreases as the axial force increases. Furthermore, as the radius becomes very small, the force becomes very large, so that an infinite force would be required to make the radius zero.

Let us consider how this relationship affects the form of Eq. 21, from which the relationship between force and tether growth rate is obtained. Given a value of the force F , and the actual values for F_0 and λ , Eq. 21 can be used to find the corresponding value of G . Recall that F_0 represents the following product (Eq. 20): $F_0 = \pi \Delta P r_t R_v$, where r_t is the tether radius when the axial force is F . If the tether radius is a function of the axial force, this quantity (F_0) is not equal to the force at which tether growth is observed to stop, since the observed force of zero tether growth, F_0^0 , occurs at a different tether radius. According to Eq. 12,

$$F_0^0 = \pi \Delta P r_t^0 R_v \quad (24)$$

where r_t^0 is the tether radius when the tether growth rate is zero. F_0 and F_0^0 are related by the ratio of the two tether radii:

$$F_0/F_0^0 = r_t/r_t^0 \quad (25)$$

If the force and the tether radius are inversely related (Eq. 23), the ratio of the two tether radii will be inversely related to the ratio of the applied force to the force when tether growth is zero, F/F_0^0 . We define the quantity

$$Q \equiv F/F_0^0 = r_t^0/r_t \quad (26)$$

F_0 is related to F_0^0 by the factor Q ,

$$F_0 = F_0^0 Q \quad (27)$$

TABLE II
DEPENDENCE OF $G^\circ(Q)$ ON λ° AND THE FLUID FORCES

Q	Fluid forces included				Fluid forces neglected			
	$\lambda^\circ = 10$	50	500	5,000	10	50	500	5,000
1.0	0.00	0.00	0.00	0.00	0.00	0.00	0.00	0.00
1.1	0.56	0.61	0.60	0.60	0.62	0.60	0.60	0.60
1.3	1.85	1.86	1.86	1.86	1.92	1.86	1.86	1.86
1.5	3.23	3.26	3.26	3.26	3.35	3.26	3.26	3.26
1.7	4.83	4.89	4.89	4.89	5.05	4.90	4.89	4.89
2.0	7.83	8.03	8.00	8.00	8.33	8.02	8.00	8.00
2.5	15.0	15.7	15.6	15.6	16.6	15.7	15.6	15.6
3.0	25.5	27.0	27.0	27.0	29.2	27.2	27.0	27.0

We would like to express the parameters of the equation of the surface (Eq. 21) in terms of observable quantities, namely F_o° . We make the following definitions:

$$G^\circ \equiv \frac{8\pi\eta v_v}{F_o^\circ} \quad (28a)$$

$$\lambda^\circ \equiv R_v/r_t^\circ = \lambda/Q. \quad (28b)$$

Substituting these quantities in Eq. 21 we have:

$$\frac{dy}{d\tilde{r}} = \frac{y}{\tilde{r}} \cdot \frac{Q^2 - \tilde{r}^2/Q\lambda^\circ}{Q^2 + \tilde{r}^2/Q\lambda^\circ} - \frac{G^\circ \cdot Q}{Q^2 + \tilde{r}^2/Q\lambda^\circ} \frac{(y^2 - 1)^{1/2}}{y\tilde{r}^2}. \quad (29)$$

The boundary conditions are

$$y = 1 \text{ at } \tilde{r} = 1 \quad (30a)$$

and

$$y = 1 \text{ at } \tilde{r} = Q\lambda^\circ. \quad (30b)$$

The method of solution is the same as that used for Eq. 21. For a given value of Q , the value of G° is found that satisfies both boundary conditions. As in the case where r_t was assumed constant, the value obtained for G° was insensitive to the value of λ° for values of $\lambda^\circ > 50$ (Table II). The functional relationship between Q and G° is shown in Fig. 3. In this case the value of G° is very close to Q^3 for values of $Q > 1.5$.

DISCUSSION

So far, no consideration has been given to possible constraints on the problem owing to the availability of surface area for incorporation into the tether or changes in the volume of the vesicle which might accompany tether formation. If the vesicle is perfectly spherical and if the surface area is constant, the volume of the vesicle must decrease as the surface is incorporated into the tether. Initially it was thought that this might be accomplished by movement of water across the membrane. However, a simple calculation shows that the driving force is not large enough to move water out of the vesicle at a sufficient rate.

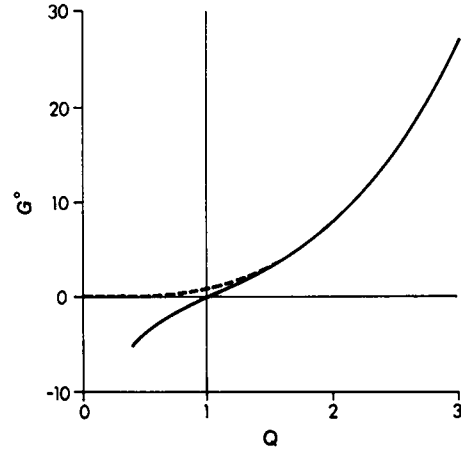


FIGURE 3 Graphic representation of the dimensionless tether growth parameter, G° , as a function of the force ratio Q . The radius of the tether is assumed to be inversely proportional to the axial force, F . The dotted line represents the curve, $G^\circ = Q^3$. The function approaches this curve for values of $Q > 1.5$.

Consider the example of a spherical vesicle of radius, $R_v = 10.0 \mu\text{m}$, forming a tether of radius, $r_t = 10.0 \text{ nm}$. For the sake of simplicity we will assume that the volume of the tether is negligible. Suppose that the length of the tether is $100 \mu\text{m}$. The area of the tether is

$$A_t = 2\pi r_t L \approx 6 \times 10^{-8} \text{ cm}^2 \quad (31a)$$

The area of the vesicle is

$$A_v = 4\pi R_v^2 \approx 12 \times 10^{-6} \text{ cm}^2. \quad (31b)$$

Thus, the area required to form the tether is only $\sim 0.5\%$ of the area of the vesicle. For a sphere, a 0.5% decrease in surface area requires a 0.75% decrease in volume. The volume of the vesicle is

$$V_v = 4/3\pi R_v^3 \approx 4 \times 10^{-9} \text{ cm}^3. \quad (32)$$

Therefore, the volume of water that must be moved out of the vesicle to form the tether (ΔV_v) is $3 \times 10^{-11} \text{ cm}^3$.

The flux of water through the membrane is the volume of water crossing the membrane per unit area per unit time:

$$J = \frac{1}{A_v} \frac{\Delta V_v}{\Delta t}. \quad (33)$$

Tether growth rates on the order of $33.0 \mu\text{m/s}$ are commonly observed (Waugh, 1982). At this rate it would take $\sim 3 \text{ s}$ to form a tether $100/\mu\text{m}$ in length ($\Delta t = 3.0 \text{ s}$). The flux of water out of the vesicle in our example would have to be

$$J \approx 10^{-6} \text{ cm/s}.$$

Let us estimate the permeability of the surface that would be necessary for such a flux to occur under the

conditions of the experiment. The relationship between the flux and the permeability is (Fettiplace and Haydon, 1980):

$$J = \frac{P_m \cdot \bar{V}_w}{R_g T} \Delta P, \quad (34)$$

where P_m is the permeability of the membrane, \bar{V}_w is the partial molar volume of water (18 cm³/mol), R_g is the gas constant (8.31 × 10⁷ erg/mol °K), T is absolute temperature (300° K), and ΔP is the hydrostatic pressure difference across the membrane. We can estimate ΔP from the force at static equilibrium via Eq. 12. Measurements of F_o indicate that its magnitude is ~10⁻⁶ dyn. Using the values for r_t and R_v in our example we calculate ΔP via Eq. 12:

$$\Delta P \approx 300 \text{ dyn/cm}^2.$$

Using this value in Eq. 34 we can calculate the permeability necessary to form a tether from a spherical vesicle at a rate of 33.0 μm/s:

$$P_m \approx 4.1 \text{ cm/s.}$$

This is three to four orders of magnitude larger than permeabilities that have been measured for egg-phosphatidylcholine bilayers (Fettiplace and Haydon, 1980). Clearly, if it were necessary to move water across the membrane to form tethers, tether growth rates such as have been observed (Waugh, 1982) could not occur. We can only conclude that when large tether growth rates are observed, the vesicles must be nonspherical, and there must be enough excess area to form the tether without decreasing the volume of the vesicle. It should be emphasized that the deviation from a spherical geometry need not be large, since, as we have shown, the amount of material in the tether is a small fraction of the total surface of the vesicle.

To assess the applicability of this analysis it is necessary to evaluate the assumptions that have been made. The important assumptions in the analysis are as follows:

(a) The surface behaves like a two-dimensional "Newtonian" liquid, as described in Eq. 5; the viscosity coefficient is independent of the rate of deformation.

(b) The area of the surface is constant.

(c) The dissipation in the surface is large compared with the dissipation in the adjacent fluid generated by the moving surface.

(d) The force exerted on the vesicle by the moving fluid can be calculated by Stokes's law.

(e) The fluid shear stress on the surface can be neglected in the tangential force balance (Eq. 1).

(f) The pressure difference across the vesicle surface is uniform and constant.

(g) The radius of the tether is inversely proportional to the axial force.

It is clear from observation that the behavior of a lipid bilayer is liquidlike; that is, it has no shear rigidity in the

plane of the surface. We have chosen the simplest type of two-dimensional liquid for the analysis, namely one for which the surface viscosity coefficient is independent of the rate of deformation. There is support for this choice in the data of Poskanzer and Goodrich (1975) which demonstrates the Newtonian character of stearic acid monolayers. However, the viscosity they measure for those films is two to three orders of magnitude larger than the viscosity estimated for lipid bilayers (Evans and Hochmuth, 1978), so it is not clear that their evidence is relevant. In any case, until there is evidence of a more complex relationship between the surface shear resultant and the rate of deformation, the simplest case will be assumed.

The low compressibility of the lipid bilayer has been demonstrated by the experiments of Kwok and Evans (1981), who have measured an area compressibility modulus of ~140 dyn/cm. From this data we can estimate the fractional area change in tether experiments. The magnitude of the forces needed to form a tether is on the order of 10⁻⁷–10⁻⁶ dyn. The magnitude of the pressure, ΔP , can be estimated from Eq. 12, and the tension in the membrane can be calculated from Eq. 4. For a tether radius of 10⁻⁵–10⁻⁶ cm, the tension in the membrane is on the order of 0.1 dyn/cm. The isotropic tension is assumed to be of the same order of magnitude as the meridional tension, T_m . Using the measured value of the compressibility modulus, K , and the constitutive equation for area expansion (Evans and Skalak, 1980) we estimate the fractional change in area:

$$\frac{\Delta A}{A} \approx \frac{T_m}{K} \approx 0.001. \quad (35)$$

Thus, the change in surface area is negligibly small.

To evaluate the validity of assumption (c) consider a tether formed from a vesicle in a fluid-filled tube. The radius of the tube is R_T . The fluid in the tube is motionless except for motion produced by the moving surface. To estimate the energy dissipation in the fluid, we consider the case of a cylinder of radius, a , being pulled through the center of a cylinder of radius, R_T . The energy dissipation per unit length, l , is approximately:

$$\frac{\dot{E}_f}{l} \approx \frac{2\pi\mu \langle v_m \rangle^2}{\ln(R_T/a)}, \quad (36)$$

where μ is the viscosity of the fluid and $\langle v_m \rangle$ is an average membrane velocity. The quantity, $\langle v_m \rangle$, is estimated by integrating the surface velocity over a spherical meridian from $r=R_v$ to $r=r_t$:

$$\langle v_m \rangle = \frac{\int_s v_m(s) ds}{\int_s ds} \approx \frac{4\dot{L}}{\pi} \left(\frac{r_t}{R_v} \right) \ln \left(\frac{R_v}{r_t} \right). \quad (37)$$

The quantity \dot{L} is the rate of tether growth. The dissipation in the membrane is approximately equal to the dissipation in a surface flowing over a spherical contour from $r=R_v$ to $r=r_t$:

$$\dot{E}_m \approx 4\pi \int_{r_t}^{R_v} \eta V_s^2 r ds \approx 2\pi\eta\dot{L}^2. \quad (38)$$

For assumption (c) to be correct, the ratio of the fluid dissipation to the membrane dissipation must be small. Taking the dimension, a , to be on the order of r_t ; the radius of the tube to be ~ 20 times larger than the radius of the vesicle; and the length, l , to be on the order of R_v , we can write:

$$\frac{\dot{E}_f}{\dot{E}_m} \approx \frac{5\mu r_t^2}{\eta R_v} \ll 1.0. \quad (39)$$

Typical values for these parameters are $\mu=10^{-2}$ poise, $r_t=10^{-6}$ – 10^{-5} cm, and $R_v=10^{-3}$ cm. For values of the surface viscosity as low as 2.0×10^{-7} surface poise, this condition will be satisfied.

Stokes's law for calculating the drag on a sphere is valid only for the case of creeping flow, that is, when the Reynolds number, Re , is <0.1 . In this experiment,

$$Re = \frac{2\rho R_v v_f}{\mu}, \quad (40)$$

where ρ is the density of the suspending fluid. The maximum fluid velocity, v_f , is $<10^{-2}$ cm/s, the radius of the vesicle is $\sim 10^{-3}$ cm, the fluid density is ~ 1.0 g/cm³ and the viscosity is $\sim 10^{-2}$ dyn s/cm². Therefore, $Re < 10^{-3}$, and the condition of creeping flow is easily satisfied. Undoubtedly, there will be some inaccuracy in using Stokes's equation because of disturbances in the flow due to the presence of the tether, the pipette to which the tether is attached, and the walls of the tube within which the experiment is performed. The drag on a sphere at the center of a tube is given by Happel and Brenner (1965) as,

$$F = 6\pi\mu R_v v_f K, \quad (41)$$

where

$$K = \frac{1 - 2/3(\zeta) - 0.1628\zeta^3 + \dots}{1 - 2.10443(\zeta) + 2.0888\zeta^3 + \dots}, \quad (42)$$

and, $\zeta = R_v/R_T$. To first order, K can be written:

$$K = 1.0 + 1.438\zeta + 0(\zeta^2). \quad (43)$$

For these experiments $\zeta \approx 0.04$, indicating that the correction would be $<6\%$. The effect of the presence of the pipette and tether is more difficult to assess, although intuitively it seems that the drag ought to be reduced by the presence of these disturbances. Attempts to measure the drag force directly have produced inconsistent results,

but the measured value has always been greater than what is predicted by the Stokes's drag. It appears that whatever effects there are from the tether and the pipette, they are not large enough to be measured. Therefore, Stokes's equation is the best available estimate of the force on the vesicle, and must be used until a better analysis or better measurements become available.

The validity of assumption (e) is supported by an order of magnitude analysis (Appendix). An alternative approach is to solve the problem numerically including the extra terms. The integral term in Eq. 2 makes exact solution extremely difficult since the relationship between r and θ is not known a priori. Assuming that the contour of the surface is approximately spherical, the equations for creeping flow around a sphere can be used to obtain an estimate of the integral terms. The tangential shear stress, τ , and the normal stress, p , for creeping flow around a sphere are given by Bird et al. (1960, pp. 58–59):

$$\tau = \frac{3}{2} \frac{\mu v_f}{R_v} \cos \theta \quad (44a)$$

$$p = \frac{3}{2} \frac{\mu v_f}{R_v} \sin \theta. \quad (44b)$$

Using Stokes's law for the total force on the vesicle,

$$F = 6\pi\mu R_v v_f, \quad (45)$$

the following equation of the surface can be obtained:

$$\begin{aligned} \frac{dy}{d\tilde{r}} = & (y/\tilde{r}) [Q^2(1 - Y) - \tilde{r}^2/Q\lambda^0] \\ & - \{G^0 Q(y^2 - 1)^{1/2}/y\tilde{r}^2 - Z\} \\ & \cdot [Q^2(1 - X) + \tilde{r}^2/Q\lambda^0]^{-1} \end{aligned} \quad (46)$$

where,

$$X = 1/2 \{1 - [1 - (\tilde{r}/Q\lambda^0)]^{1/2}\} \quad (47a)$$

$$\begin{aligned} Y = X - \tilde{r} \frac{dX}{d\tilde{r}} \\ = 1/2 \{1 - [1 - (\tilde{r}/Q\lambda^0)^2]^{-1/2}\} \end{aligned} \quad (47b)$$

$$Z = 1/2 \tilde{r}(\lambda^0)^{-2}(y^2 - 1)^{-1/2}. \quad (47c)$$

The quantities X and Y arise from the integral term of Eq. 2. The remaining term, Z , comes from the inclusion of the tangential shear stress in Eq. 1. Eq. 46 is subject to the same boundary conditions as before (Eq. 30), and the procedure for obtaining the dependence of G^0 on Q is also the same. The results are shown in Table II. The relationship between Q and G^0 is not significantly altered by the inclusion of these additional terms.

Assumption (f) is difficult to verify because of uncer-

tainty about the origin of the trans-membrane pressure. The existence of a stress normal to the surface is confirmed from two observations: first, the approximately spherical geometry of the vesicle, and second, the existence of a nonzero drag force at which the vesicle is stationary. It is possible that the pressure could change as a result of material being pulled from the vesicle surface as the tether grows. This can be checked experimentally by measuring the critical force as a function of tether length. Thus, assumption (f) must be re-examined in light of experimental results.

Assumption (g) was introduced to account for the possibility that the tether radius may be a function of the axial force on the tether. Unfortunately the experimental results at this time are not sufficient to establish the precise nature of the functional relationship. It may be necessary to replace the constant in Eq. 23 with some function of the radius: $F = f(r_t) \cdot 1/r_t$. There are many forms that $f(r_t)$ might take, but two extreme cases might be imagined. The first is that the relationship between F and r_t is insensitive to the magnitude of the tether radius. In this case $f(r_t)$ would be constant, and the appropriate solution for the tether growth rate would be the one shown in Fig. 3. The second case is that the force-radius relationship is a strong function of the radius. Such a situation would arise if the tether radius were limited by the packing constraints of the molecules as the radius became very small. In this case $f(r_t)$ could be approximated by a step function at some minimum value of r_t , and the assumption that the tether radius is constant would be more appropriate (Fig. 2). Thus, the two solutions presented (Fig. 2 and Fig. 3) bracket the likely behavior of a tether under an axial load. The data presented in a companion paper (Waugh, 1982) seem to favor the solution shown in Fig. 3. This indicates that a minimum tether radius has not been reached in these experiments, and that the tether radius decreases as the axial force increases.

CONCLUSIONS

A relationship has been derived by which the intrinsic surface viscosity, η , can be calculated from observable quantities in vesicle tether growth experiments. The rate of tether growth is measured as a function of the velocity of the suspending fluid. The force on the vesicle is approximated by Stokes's drag equation. The ratio of the force on the vesicle to the critical force is used to determine the dimensionless tether growth parameter via the functional relationship illustrated in Fig. 3. Knowing the tether growth parameter, the tether growth rate, and the critical force, the viscosity can be calculated from the definition of the tether growth parameter.

APPENDIX

We present here an order of magnitude analysis to show that the fluid shear forces in Eqs. 1 and 2 can be neglected without affecting the results

of the analysis. The equation of the surface including these terms is given by Eq. 46:

$$\frac{dy}{d\tilde{r}} = (y/\tilde{r})[Q^2(1 - Y) - \tilde{r}^2/Q\lambda^0] - \{G^0Q(y^2 - 1)^{1/2}/y\tilde{r}^2 - Z\} \cdot \{Q^2(1 - X) + \tilde{r}^2/Q\lambda^0\} \quad (A1)$$

The local fluid forces are contained in the terms X , Y , and Z , which are defined in Eq. 47. For the purposes of estimating the effect of these terms, the stress expressions for creeping flow around a sphere (Eq. 44a and b) have been used. The origins of the other terms in the equation are as follows:

$$Q^2(y/\tilde{r}) \quad (\text{from tether reaction force, } F_r) \quad (A2)$$

$$\tilde{r}^2/Q\lambda^0 \quad (\text{from the pressure difference, } \Delta P_r) \quad (A3)$$

$$G^0Q(y^2 - 1)^{1/2}/y\tilde{r}^2 \quad (\text{from the } (T_m - T_s) \text{ term in Eq. 1; viscous dissipation in the surface.}) \quad (A4)$$

For the purpose of estimating the various terms, it is useful to put the equation in the following form:

$$\frac{dy}{d\tilde{r}} = \frac{y^2}{\tilde{r}}(y^2 - 1)^{-1/2} \cdot \frac{F_r - F_t - F_p - F_s - F_\tau}{\text{den}} \quad (A5)$$

where

$$\text{den} = Q^2(1 - X) + \tilde{r}^2/Q\lambda^0 \quad (A6)$$

$$F_r = \text{reaction force} = Q^2(1 - y^2)^{1/2}/y \quad (A7)$$

$$F_p = \text{pressure force} = \tilde{r}^2(y^2 - 1)^{1/2}/Q\lambda^0 y \quad (A8)$$

$$F_s = \text{surface dissipation} = QG^0(y^2 - 1)/\tilde{r}y^3 \quad (A9)$$

$$F_\tau = \text{local shear stress} = \tilde{r}^2/2(\lambda^0)^2 y^2 \quad (A10)$$

$$F_t = \text{integral of fluid tractions} = Q^2Y(y^2 - 1)^{1/2}/y \\ = Q^2\{1 - [1 - (\tilde{r}/Q\lambda^0)^2]^{-1/2}\}(y^2 - 1)^{1/2}/2y. \quad (A11)$$

We wish to estimate the relative magnitudes of these terms in various regions of the deforming surface. In making the estimates we will assume that G^0 and Q are on the order of one, $O(1)$, and that λ^0 is the only large parameter. We consider three regions of the surface:

$$\text{I. } \tilde{r} = O(1)$$

$$\text{II. } \tilde{r} = O(\sqrt{\lambda^0})$$

$$\text{III. } \tilde{r} = O(\lambda^0).$$

In addition to \tilde{r} , we will also need to know the magnitude of the quantity y . From the initial and final boundary conditions we know that in regions I and III, $y = O(1)$. Because in region I, $dy/d\tilde{r}$ is also on the order of 1, in region II we must let $y = O(\tilde{r}) = O(\sqrt{\lambda^0})$.

All that remains is to evaluate the magnitude of each of the terms in each region.

Region I. $\tilde{r} = O(1)$, $y = O(1)$

$$\begin{aligned} F_r &= O(1) \\ F_p &= O(1/\lambda^0) \\ F_s &= O(1) \\ F_\tau &= O(1/\lambda^0) \\ F_f &= O(1/\lambda^0) \\ \text{den} &= Q^2 \end{aligned}$$

Region II. $\tilde{r} = O(\sqrt{\lambda^0})$, $y = O(\sqrt{\lambda^0})$

$$\begin{aligned} F_r &= O(1) \\ F_p &= O(1) \\ F_s &= O(1/\lambda^0) \\ F_\tau &= O(1/\lambda^0) \\ F_f &= O(1/\lambda^0) \\ \text{den} &\approx Q^2 + \tilde{r}/Q\lambda^0 \end{aligned}$$

Region III. $\tilde{r} = O(\lambda^0)$, $y = O(1)$

$$\begin{aligned} F_r &= O(1) \\ F_p &= O(\lambda^0) \\ F_s &= O(1/\lambda^0) \\ F_\tau &= O(1) \\ F_f &= O(1) \\ \text{den} &\approx \tilde{r}^2/Q\lambda^0 \end{aligned}$$

In region I (near the tether) the axial force, F , and the viscous dissipation in the surface dominate the equation. In region II the axial force and the pressure force are important, and in region III only the pressure force is large. In all regions the fluid tractions (F_f and F_τ) can be neglected, and the denominator can be written: $\text{den } Q^2 + \tilde{r}/Q\lambda^0$. Thus, all of the terms, X , Y , and Z , arising from the integral in Eq. 2 and the surface traction, $r\tau$, in Eq. 1 can be neglected in all of the regions.

The author would like to thank Dr. Evan Evans for suggesting this problem and for his comments on the force-dependence of tether radius, Dr. Alfred Clark for his contribution of the order of magnitude analysis (appendix) and his comments on drag force calculations, and Dr. Giles Cokelet for his in-house review.

This work was supported in part by National Institutes of Health grants HL-07152 and HL-16421. This paper is based on work performed under contract No. DE-AC02 76EVO3490 with the U.S. Department of Energy at the University of Rochester Department of Radiation Biology and Biophysics, and has been assigned Report No. UR-3490-1957.

Received for publication 26 January 1981 and in revised form 2 June 1981.

REFERENCES

- Bird, R. B., W. E. Stewart, and E. N. Lightfoot. 1960. Transport Phenomena. John Wiley & Sons, Inc., New York. 56-58.
- Evans, E. A., and R. M. Hochmuth. 1976. Membrane viscoplastic flow. *Biophys. J.* 16:13-26.
- Evans, E. A., and R. M. Hochmuth. 1978. Mechanochemical properties of membranes. *Curr. Top. Membr. Transp.* 10:1-62.
- Evans, E. A., and R. Skalak. 1980. Mechanics and Thermodynamics of Biomembranes. CRC Press, Inc., Boca Raton, FL. 1-254.
- Fettiplace, R., and D. A. Haydon. 1980. Water permeability of lipid membranes. *Physiol. Rev.* 60:510-550.
- Happel, J., and H. Brenner. 1965. Low Reynolds Number Hydrodynamics. Prentice-Hall, Inc., Englewood Cliffs, NJ. 318.
- Hochmuth, R. M., N. Mohandas, and P. L. Blackshear, Jr. 1973. Measurement of the elastic modulus for red cell membrane using a fluid mechanical technique. *Biophys. J.* 13:747-762.
- Kwok, R., and E. A. Evans. 1981. Thermoelasticity of large lecithin bilayer vesicles. *Biophys. J.* 35:637-652.
- Poskanzer, A., and F. C. Goodrich. 1975. A new surface viscometer of high sensitivity. II. Experiment with stearic acid monolayers. *J. Colloid Interface Sci.* 52:213-221.
- Waugh, R. E. 1982. Surface viscosity measurements from large bilayer vesicle tether formation. II. Experiments. *Biophys. J.* 38:29-37.